

**On the Synthesis of new four-layered Aurivillius
compound $\text{Bi}_2\text{MNa}_2\text{Nb}_4\text{O}_{15}$ (M= Ca, Sr, Ba)**

A Thesis Submitted in Partial Fulfillment of the
Requirements for the Degree of

Bachelor of Technology
By

Anubhav Das

Roll no: 107CR032



Department of Ceramic Engineering.
National Institute of Technology, Rourkela, Odisha.

**On the Synthesis of new four-layered Aurivillius
compound $\text{Bi}_2\text{MNa}_2\text{Nb}_4\text{O}_{15}$ (M= Ca, Sr, Ba)**

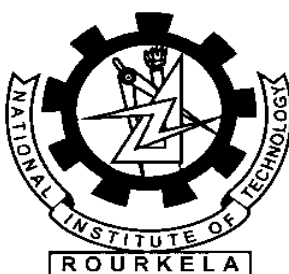
A Thesis Submitted in Partial Fulfillment of the
Requirements for the Degree of

Bachelor of Technology
By

Anubhav Das

Roll no: 107CR032

Supervisor: **Dr. JAPES BERA**



Department of Ceramic Engineering.
National Institute of Technology, Rourkela, Odisha.

ACKNOWLEDGEMENTS

With deep regards and profound respect, I take this opportunity to express my deep sense of gratitude and indebtedness to Prof. Japes Bera, Head of the Department, Department of Ceramic Engineering, N. I. T. Rourkela, for introducing the research topic and for his inspiring guidance, constructive criticism and valuable suggestion throughout this research work. It would have not been possible for me to bring out this project report without his constant help and encouragement. I wish that he will keep in touch with me in future and will continue to give his valuable advice.

I am also grateful to all the faculties of Department of Ceramic Engineering, whose vast knowledge in the field of Ceramics has enlightened me in different areas of this research work.

I am also thankful to Miss. Arundhati Chakrabarti, Miss Geetanjali Parida and other research scholars in Department of Ceramic Engineering for providing the joyful environments in the lab and helping me. It was a nice and memorable experience with all the things of my department. I wish to give them my heartfelt thanks for their constant help and support.

I would also like to thank my parents for constantly encouraging and supporting me to give my 100 % and work hard till I achieve my goal.

Above all, I thank the Almighty GOD for giving me all these people to help and encourage me, and for the skills and opportunity to complete this report.

Date:

Anubhav Das



National Institute of Technology Rourkela

CERTIFICATE

This is to certify that the thesis entitled, “*Synthesis of new four-layered Aurivillius compounds $Bi_2MNa_2Nb_4O_{15}$ ($M= Ca, Sr, Ba$)*” submitted by Mr. **Anubhav Das** in fulfillment for the requirements for the award of **Bachelor of Technology** degree in **Ceramic Engineering** at National Institute of Technology, Rourkela is an authentic work carried out by him under my supervision and guidance.

To the best of my knowledge, the matter embodied in the thesis has not been submitted to any other University/ Institute for the award of any Degree or Diploma.

Date:

Dr. Japes Bera
(Head of the Department)
Dept. of Ceramic Engineering
National Institute of Technology
Rourkela-769008

CONTENTS

PAGE No

I. List of Figures.....	1-2
II. Abstract.....	3-4
1. Introduction.....	5-7
2. Literature Review.....	8-13
2.1 General Introduction	
2.2 Recent Developments	
2.3 Summary	
3. Experimentation.....	14-18
3.1 Experimental Procedure	
3.2 Flow Chart	
3.3 Sample Characterization	
4. Results and Discussions.....	19-29
4.1 Thermal Decomposition	
4.2 Phase formation Behavior	

CONTENTS

PAGE No

5. Conclusion.....30-31

6. Reference.....32-36

LIST OF FIGURES

1. Figure 1: Crystal structure of the four layered Aurivillius phase $\text{Bi}_2\text{SrNa}_2\text{Nb}_4\text{O}_{15}$. [Page no: 12]
2. Figure 2: Flow chart for the synthesis of the four layer Aurivillius phase. [Page no: 17]
3. Figure 3: TG-DSC curves for $\text{Bi}_2\text{BaNa}_2\text{Nb}_4\text{O}_{15}$ precursor powder. [Page no:20]
4. Figure 4: TG-DSC curves for $\text{Bi}_2\text{CaNa}_2\text{Nb}_4\text{O}_{15}$ precursor powder. [Page no:21]
5. Figure 5: TG-DSC curves for $\text{Bi}_2\text{SrNa}_2\text{Nb}_4\text{O}_{15}$ precursor powder. [Page no: 22]
6. Figure 6: The XRD pattern of $\text{Bi}_2\text{BaNa}_2\text{Nb}_4\text{O}_{15}$ precursor powder and the precursor calcined at 800°C and 900°C respectively. [Page no: 23]
7. Figure 7: The XRD pattern of $\text{Bi}_2\text{BaNa}_2\text{Nb}_4\text{O}_{15}$ precursor powder along with the precursor calcined at 1000°C , 1050°C and 1100°C respectively. [Page no: 24]

8. Figure 8: The XRD pattern of $\text{Bi}_2\text{CaNa}_2\text{Nb}_4\text{O}_{15}$ precursor powder and the precursor calcined at 800°C and 900°C respectively. [Page no: 26]
9. Figure 9: The XRD pattern of $\text{Bi}_2\text{CaNa}_2\text{Nb}_4\text{O}_{15}$ precursor powder and the precursor calcined at 1000°C , 1050°C and 1100°C respectively. [Page no: 27]
10. Figure 10: The XRD pattern of $\text{Bi}_2\text{SrNa}_2\text{Nb}_4\text{O}_{15}$ precursor powder and the precursor calcined at 800°C and 900°C respectively. [Page no: 28]
11. Figure 11: The XRD pattern of $\text{Bi}_2\text{SrNa}_2\text{Nb}_4\text{O}_{15}$ precursor powder and the precursor calcined at 1000°C , 1050°C and 1100°C respectively. [Page no: 29].

ABSTRACT

ABSTRACT:

The aim of the project was to synthesize $\text{Bi}_2\text{MNa}_2\text{Nb}_4\text{O}_{15}$ (M= Ca, Sr, Ba) by the Oxalate route. The detailed analysis of the DSC-TG plot depicted that the working range of calcination must be within 1000°C . However due to presence of competing secondary phases like BiNbO_4 , the synthesis of pure phase material was not possible. The detailed analysis that favored this fact was supported by powder X-ray diffraction (XRD). The precursor powder obtained was calcined at 800°C , 900°C , 1000°C , 1050°C and 1100°C , respectively. And the XRD analysis showed that as long as there was BiNbO_4 in the system there were very negligible chances of preparation of the desired phase.

CHAPTER 1

INTRODUCTION

Introduction:

Aurivillius phase [1-3] is a group of compounds and the majority of them exhibit ferroelectric behavior at room temperature. The bismuth layer structured ferroelectrics have attracted a remarkable interest over the past decade due to rich variety of technologically important properties exhibited by such materials [4-8].

Majority of these oxides are normal ferroelectrics with fairly high Curie temperature as a result of formation of a short bond between the apex oxygen in the perovskite layer and the bismuth in the $[\text{Bi}_2\text{O}_2]^{2+}$ layer associated with octahedral rotations and cationic displacements [9]. These also have got potential application in non-volatile random access memory [NVRAM] and high temperature piezo-electrics [10, 11].

One of the interesting features of this Aurivillius phase is the compositional flexibility of the perovskite sets or blocks which allows to incorporate various cations such as Na^+ , K^+ , Ca^{2+} , Sr^{2+} , Ba^{2+} , Bi^{3+} and many more for A-site and Fe^{3+} , Cr^{3+} , Ti^{4+} , Nb^{5+} , W^{6+} for B-site. Thus it is possible to modify the properties according to the chemical composition.

Structural studies of the Aurivillius phase reveal that the $[\text{Bi}_2\text{O}_2]^{2+}$ layers that are interwoven with perovskite like $[\text{A}_{n-1}\text{B}_n\text{O}_{3n+1}]^{2-}$ layers. Here the B-site cation resides in the interstitial site of the octahedron of oxygen anions. The perovskite unit-cell is built to form corner sharing BO_6 octahedrons that are connected through B-O-B linkages. The A-site cations fit into the large cavity of the center of eight cornered sharing BO_6 octahedron $[\text{A}_{n-1}\text{B}_n\text{O}_{3n+1}]$ denotes the perovskite like slabs derived by the termination of the three-dimensional ABO_3 perovskite structure along the (100) axis which are interlinked with $[\text{Bi}_2\text{O}_2]^{2+}$ fluorite type structure giving a characteristic layered structure.

Depending on the choice and stoichiometry of A and B site ions aurivillius structure oxides can possess a wide variety of interesting properties. Aurivillius phase are non-centrosymmetric giving rise to ferroelectricity making them applicable for nonvolatile memory applications [12]. Aurivillius phases have also found other properties and applications such as photoluminescence device [13], ion exchange and intercalation behavior [14-16] and the possibility of combining d^n and d^0 transition metal ions for the realization of multiferroelectric properties [17, 18]. *Kim* has found that 2-layer Aurivillius phase $\text{Bi}_2\text{PbNb}_2\text{O}_9$; it was an excellent photocatalyst working under visible light in 2004 [19]. There has been growing interest in the study of Aurivillius phases which may be potential photocatalytic material in future [20, 21].

For example- a typical series of aurivillius phases $\text{Bi}_2\text{Mo}_n\text{O}_{3n+3}$ ($1 \leq n \leq 3$) had a photocatalytic activity oxygen evolution and could degrade organic compounds under visible light irradiation [22-24]. Recently there are several groups that have prepared one layered aurivillius phases Bi_2WO_6 nano-plates and nano-flowers to investigate their visible-light-driven photocatalytic activities [25-28]. These works revealed that Bi_2WO_6 could perform as an excellent photocatalytic material and solar-energy-conversion material.

CHAPTER 2

LITERATURE REVIEW

2 Literature review:

2.1 General Introduction

The family of bismuth oxides was discovered over 50 years by Aurivillius [3]. Recently the interest in the properties of the Aurivillius as temperature stable ferro-piezoelectrics has been increased. Many bismuth layered crystals and their crystals have been analyzed in detail. Maximum of these materials are normal ferroelectrics with a fairly high curie temperature, while only few of them such as $\text{BaBi}_2\text{NbO}_9$, $\text{BaBi}_2\text{Ta}_2\text{O}_2$ etc. show relaxor behavior [29-31].

The structural evolution in three and four layer Aurivillius solid solution in which a comparative study versus relaxor properties have been reported by *Jenny Tellier et.al* [32] in which two solid solutions of three layers $\text{Ba}_x\text{Bi}_{4-x}\text{Nb}_x\text{Ti}_{3-x}\text{O}_{12}$ ($0 < x \leq 1.2$) and four layered Aurivillius compounds $(\text{Na}_{0.5}\text{Bi}_{0.5})_{1-x}\text{Ba}_x\text{Bi}_4\text{TiO}_{15}$ were synthesized by solid state reaction. The evolution of their crystal structures as a function of x was performed using Rietveld refinements from XRD data. The relaxor behavior was observed for samples whose tolerance value was greater than 0.96.

Analysis was done for dielectric material. *A.V. Murugan et.al* carried the synthesis of nano crystalline ferroelectric $\text{BaBi}_4\text{Ti}_4\text{O}_{15}$ (BBT) by Pechini method [33]. A gel was made by using aqueous solution of BaCl_2 , BiNO_3 , TiOCl_2 and citric acid in stoichiometric ratio and was heated in a waterbath. The gel showed decomposition behavior at 600°C and produced nano crystallites of ternary oxide BBT. The phase contents and lattice parameters were analyzed by powder XRD and the particle size by TEM. The room temperature dielectric constant was found to be around 90 at 1 KHz.

Nano-scaled BBT powder was also synthesized by sol-gel method by *Dan Xie et.al* [34]. Here the BBT powders were synthesized from barium acetate, barium nitrate and tetrabutyl titanate.

The bismuth layered perovskite structure of BBT was formed at 750°C. Its granularity distribution is centralized from 150-180 nm and the average particle size was 160 nm.

The electrical properties of donor- and acceptor- doped $\text{BaBi}_4\text{Ti}_4\text{O}_{15}$ were studied by *Irene Pribosic et.al* [35] and they prepared samples by reaction sintering of a mixture of BaTiO_3 and $\text{Bi}_4\text{Ti}_3\text{O}_{12}$ with Nb substituted Ti as a donor dopant and Fe acts as acceptor dopant. The dielectric constant of BBT was increased by both the dopants because Nb doping decreased the Curie temperature and Fe increased it. The conductivity of BBT was found to be p-type and was decreased by Nb doping.

Later a comparative study of the Aurivillius phase ferroelectrics i.e. $\text{CaBi}_4\text{TiO}_{15}$ and $\text{BaBi}_4\text{TiO}_{15}$ was carried out by *J.Tellier et.al* [36]. These phases were analyzed by single crystal XRD. A significant deformation of perovskite was observed when $\text{CaBi}_4\text{Ti}_4\text{O}_{15}$ was compared with respect to the tolerance factor. The rotation system of $\text{CaBi}_4\text{Ti}_4\text{O}_{15}$ is typical from even larger Aurivillius phase and uses space group $A2_1am$. For the case of $\text{BaBi}_4\text{Ti}_4\text{O}_{15}$ only a weak variation to the $F2am$ space group can be found out by single crystal XRD.

The substitution of La^{3+} was carried in the four layer Aurivillius phase $\text{SrBi}_4\text{Ti}_4\text{O}_{15}$ by *R.Z Hou* and co-workers [37]. The ceramics with composition of $\text{SrBi}_{4-x}\text{La}_x\text{Ti}_4\text{O}_{15}$ was prepared within the range ($0 < x \leq 1.8$) and the dielectric properties were tested. Single phase $\text{SrBi}_{4-x}\text{La}_x\text{Ti}_4\text{O}_{15}$ solid solution exists when $x=1.6$ and the secondary phase of $\text{Li}_{2/3}\text{TiO}_3$ appears. The Curie temperature which was 520°C for $\text{SrBi}_4\text{Ti}_4\text{O}_{15}$ shifts to a lower temperature when x is increased because smaller structural distortion is caused by La^{3+} substitution. Here no dielectric behavior was observed.

Cation disorder and phase transition in the four layer ferroelectric Aurivillius phase $ABi_4Ti_4O_{15}$ (A=Ca, Sr, Ba, Pb) was observed by B.J. Kennedy and his co-workers [38]. In this comparative study the crystal structures have been studied by combination of synchrotron X-rays and neutron powder diffraction data. All these four oxides attain an orthorhombic structure at room temperature and their structures have been refined at space group $A2_1am$. This structure is a result of rotation of TiO_6 resulting from less than desired size of A-type cation and displacement of Ti atoms towards the Bi_2O_2 layer. Partial disorder was also seen between Bi and A-type cation over the two of the three available sites which increases in the order $Ca < Sr$ and $Pb < Ba$.

Aurivillius phase with triple layered perovskite like slabs $[A_2B_3O_{10}] Bi_2ANaNb_3O_{12}$ (A=Sr, Ca) and $Bi_2CaNaNb_3O_{12}$ have been synthesized by *Sugara* and co-workers [39]. After that they developed a novel method for getting protonated forms of layered perovskites derived from Aurivillius phases through acid treatment of $Bi_2SrNaNb_3O_{12}$ and $Bi_2CaNaNb_3O_{12}$ [40]. This is done by selective leaching of the bismuth oxide sheets and correspondingly introduction of protons for charge compensation. The main aim of the reaction was to substitute bismuth oxide sheets with protons without changing the perovskite-slab like structure. Then the photocatalytic activity of the triple layered Aurivillius phases was performed. The $Bi_2ANaNb_3O_{12}$ (A=Sr, Ca) and $Bi_2CaNaNb_3O_{12}$ were prepared from the Aurivillius phases through selective leaching of the bismuth sheets. They found the catalytic activity for H_2 evolution was elevated after selective leaching of bismuth oxide sheets.

2.2 Recent Developments:

Associated work done with respect to my project is the synthesis of $Bi_2SrNa_2Nb_4O_{15}$ in solid-oxide route by *Zhenhua Liang et.al* [41] in which the B-site was fully occupied by the niobium

ions. Detailed XRD study of $\text{Bi}_2\text{SrNa}_2\text{Nb}_4\text{O}_{15}$ showed that the phase crystallizes in the space group $I4/mmm$.

By using 6M HCl at room temperature the protonated forms were investigated easily. The structure and compositions of the protonated forms as well as the mechanisms of the conversion reactions were analyzed. The following figure shows the diagram of the crystal structure of the four layered Aurivillius phase $\text{Bi}_2\text{SrNa}_2\text{Nb}_4\text{O}_{15}$.

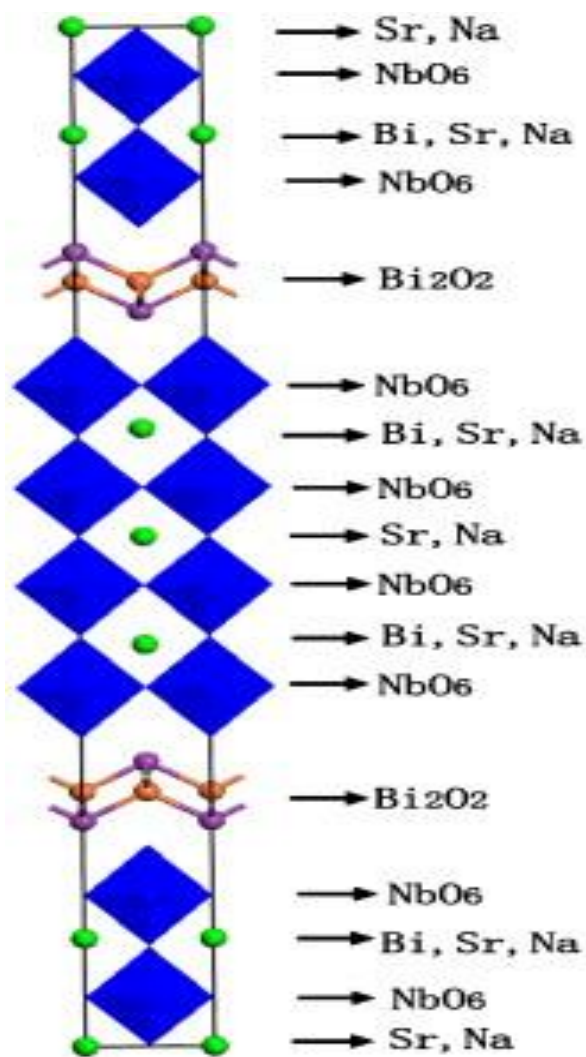


Figure 1: Crystal structure of the four layered Aurivillius phase $\text{Bi}_2\text{SrNa}_2\text{Nb}_4\text{O}_{15}$.

2.3 Summary of the literature:

From the literature review it is found that there is no report on the synthesis of the new $\text{Bi}_2\text{MNa}_2\text{Nb}_4\text{O}_{15}$ (M= Ca, Sr, Ba) Aurivillius phase by the Oxalate route. This provides a wide scope, suggesting carrying out work in this route and synthesizing the materials and its characterization.

CHAPTER 3

EXPERIMENTATION

3. Experimental

3.1 Experimental Procedure:

All the reagents that were used were analytically pure. Polycrystalline powders of $\text{Bi}_2\text{MNb}_2\text{Nb}_4\text{O}_{15}$ (M= Ca, Sr, Ba) Aurivillius phase were prepared by Oxalate precipitation route. The required batch calculations were done and necessary reagents were then weighed to prepare a final batch of 5 grams of the required sample.

Here M = Ca, Sr, Ba.

For M= Ba

First 3.9993gm of $\text{Bi}(\text{NO}_3)_3 \cdot 5\text{H}_2\text{O}$ was weighed and added with 10.5 cc of HNO_3 and placed on magnetic stirrer for stirring. Then 1.0773 gm. of $\text{Ba}(\text{NO}_3)_2$ was weighed and added with 123.5cc of water and stirred. When the above salt was completely dissolved, 0.7007gm of NaNO_3 was added to the aqueous solution of barium nitrate for complete dissolution. The bismuth nitrate solution was then added drop-wise to the barium- and sodium nitrate and stirred for uniform mixing. Next a solution of 2.8584 gm of oxalic acid was prepared in 52cc of water. To this 2.1915gm of Nb_2O_5 was added to form a suspension. This suspension was then ultrasonicated for 15 mins to break the soft agglomerates.

The previously prepared mixed nitrate solution was added drop wise into the suspension of oxalic acid and Nb_2O_5 . This precipitates barium, bismuth and sodium oxalates into the Nb_2O_5 -oxalic acid suspension. Then ammonia was added until the pH of the solution was adjusted to 7. The precipitated solution was aged for 24h for complete precipitation. The precipitate was

filtered and the filtrate was washed with distilled water and isopropyl alcohol. Finally the powder was dried at 70°C.

The raw material thus obtained was analyzed by DSC-TG and XRD. The precursor powder was calcined at 800°C, 900°C, 1000°C, 1050°C and 1100°C and its XRD analysis was performed for further progress.

Similar procedure was carried out for the synthesis of $M = \text{Ca, Sr}$ and were characterized as stated above.

3.2 Flow diagram for the synthesis of the sample:

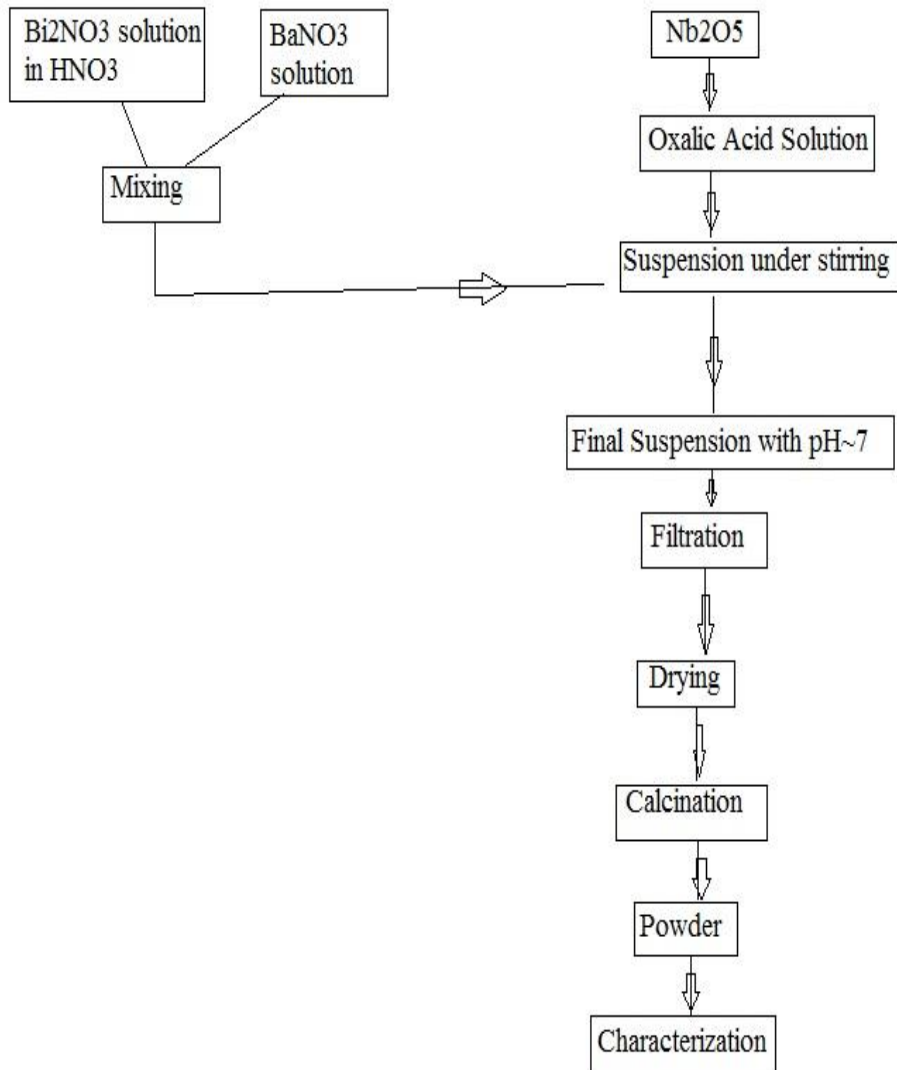


Figure 2: Flow chart of the whole process for the synthesis of the Aurivillius layer.

3.3 Sample Characterization

3.3.1 Thermal Decomposition:

The precursors prepared by oxalate precipitation route were characterized for its thermal decomposition behavior using NETZSCH-TG DSC machine having Model No: 409C in the temperature range of room temperature to 1000°C at 10°C/min.

3.3.2 Phase Characterization:

The raw and calcined powder was characterized for its phase identification using X-Ray Diffraction analysis in Phillips XRD Machine having Model no: PW-1830, Phillips, Netherlands using Copper $K\alpha$.

CHAPTER 4

RESULTS & DISCUSSION

4.1 Thermal Decomposition

4.1.1 Thermal Decomposition behaviour of $\text{Bi}_2\text{BaNa}_2\text{Nb}_4\text{O}_{15}$

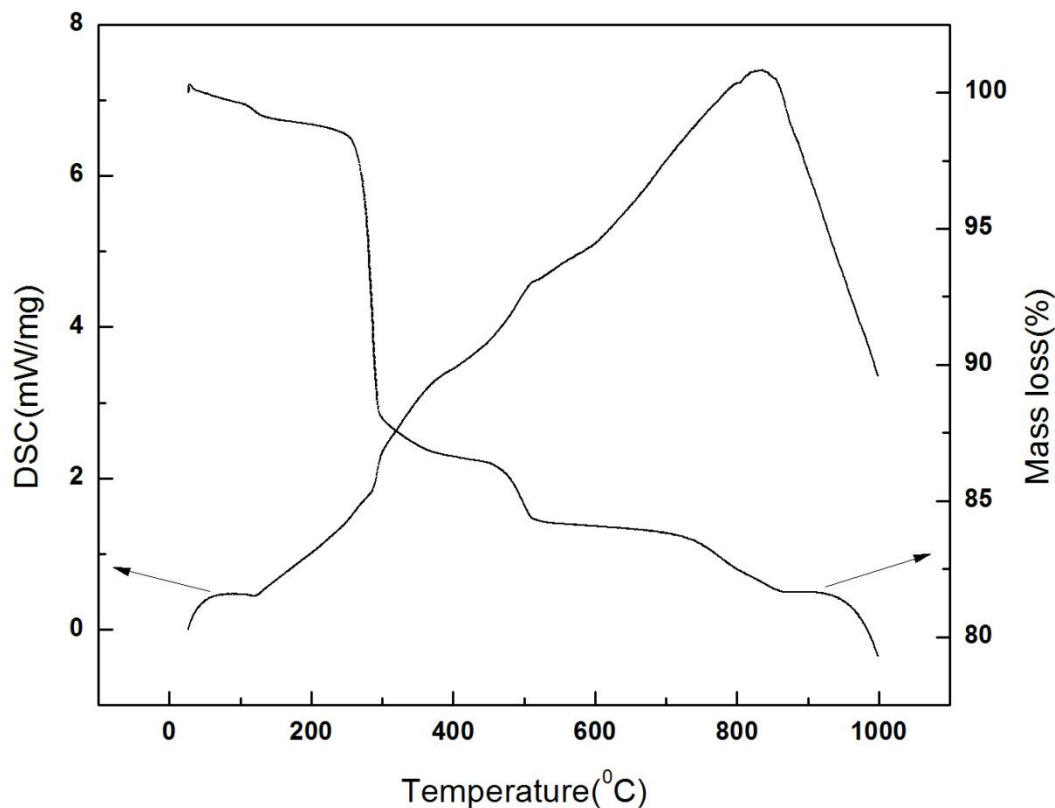


Figure 3: TG-DSC curves for $\text{Bi}_2\text{BaNa}_2\text{Nb}_4\text{O}_{15}$.

Fig.3 shows the TG-DSC curves for $\text{Bi}_2\text{BaNa}_2\text{Nb}_4\text{O}_{15}$ precursor powder. Weight loss occurs in four stages in the sample in the temperature range 200-400°C, 400-600°C, 600-900°C, and 900-1000°C. Initial weight loss in the sample was due to loss of moisture from the sample. The second step in weight loss may be due to decarboxylation of oxalate hydrate phases.

The third and fourth stage weight loss was due to the decomposition of mainly barium carbonate (BaCO_3). The barium carbonate was formed as an intermediate compound from the decomposition of barium oxalate. This has been reported earlier by *Chakrabarti.A et al.* in Dielectric properties of $\text{BaBi}_4\text{Ti}_4\text{O}_{15}$ ceramics produced by cost-effective chemical method [42].

Studying the DSC-TG graph it can be found out that the decarboxylation of oxalates was an exothermic reaction and while the carbonate decomposition was an endothermic reaction.

4.1.2 Thermal Decomposition of $\text{Bi}_2\text{CaNa}_2\text{Nb}_4\text{O}_{15}$.

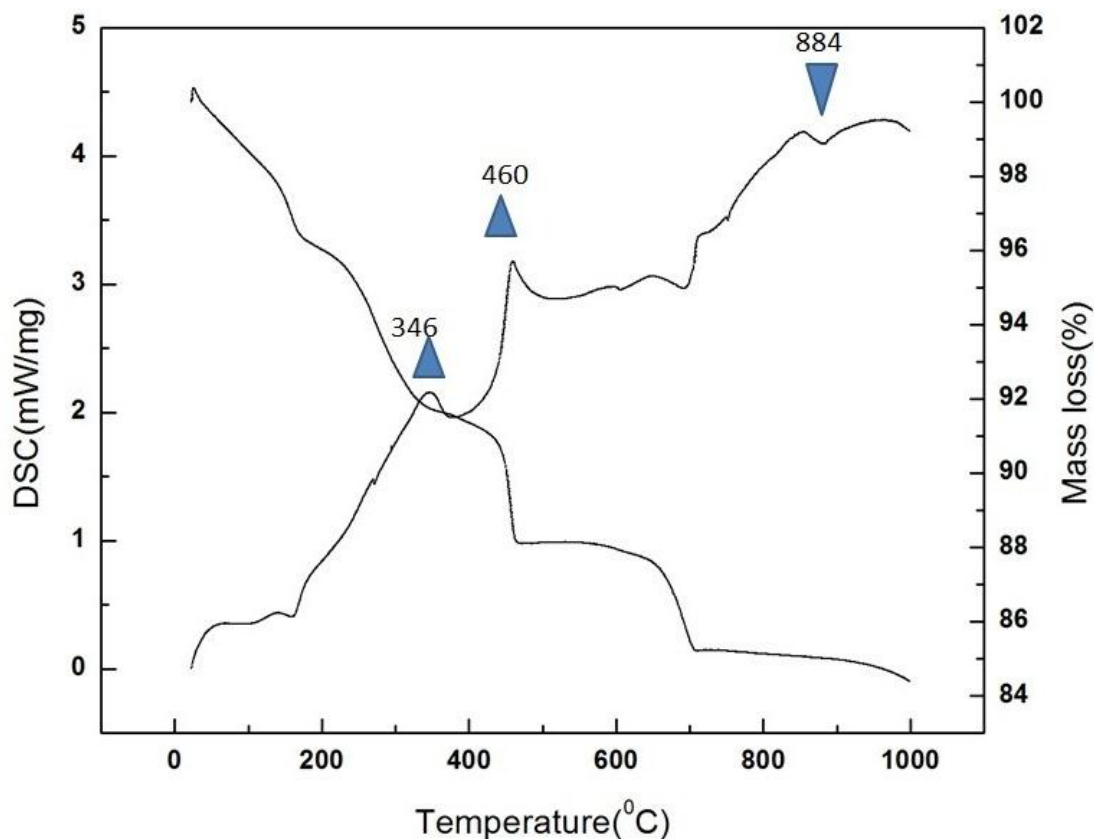


Figure 4: DSC-TG curves for $\text{Bi}_2\text{CaNa}_2\text{Nb}_4\text{O}_{15}$ precursor powder.

Fig.4 shows the DSC curves for $\text{Bi}_2\text{CaNa}_2\text{Nb}_4\text{O}_{15}$ precursor powder. This plot shows that there were three stages of decomposition in the temperature range 300-450°C, 450-700°C and 700-1000°C.

The first and second stage corresponded to two exothermic reactions with peak at 346°C and 460°C. These were due to decarboxylation of bismuth oxalate and calcium oxalates, respectively.

The third weight loss corresponds to endothermic reaction at 884°C due to decomposition of CaCO_3 . This has been reported by J.Bera et.al [42]. There was an endothermic peak at 884°C due to the crystallization of phase.

4.1.3 Thermal Decomposition of $\text{Bi}_2\text{SrNa}_2\text{Nb}_4\text{O}_{15}$.

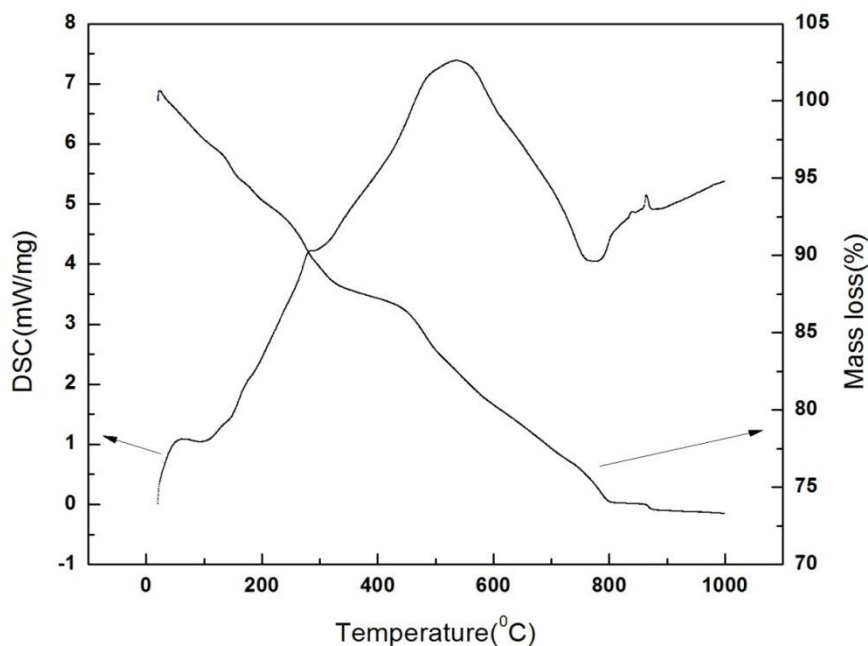


Figure 5: DSC-TG curves for $\text{Bi}_2\text{SrNa}_2\text{Nb}_4\text{O}_{15}$ precursor powder.

Figure 5: TG-DSC curves for $\text{Bi}_2\text{SrNa}_2\text{Nb}_4\text{O}_{15}$ precursor powder.

Figure 5 shows the TG-DSC curves for $\text{Bi}_2\text{SrNa}_2\text{Nb}_4\text{O}_{15}$ precursor powder. Approximately it has three stages of weight losses. The first and second stage of weight losses corresponded to the exothermic peaks. This was due to the decarboxylation of bismuth oxalate and strontium oxalate, respectively. The third weight loss was due to decomposition of strontium carbonate. This reaction is endothermic reaction. This has been reported by J.Bera et.al [42].

4.2 Phase Formation Behavior:

The phase formation behavior during calcination was studied by evaluating the phase formed in the specimen using XRD.

4.2.1 Phase formation behavior of $\text{Bi}_2\text{BaNa}_2\text{Nb}_4\text{O}_{15}$.

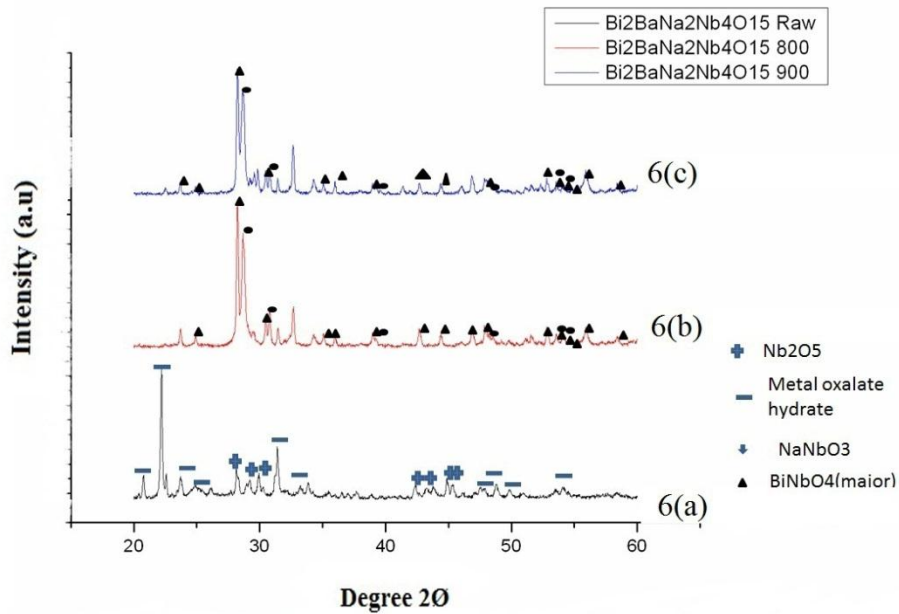


Figure 6: The XRD pattern of $\text{Bi}_2\text{BaNa}_2\text{Nb}_4\text{O}_{15}$ precursor powder and the precursor calcined at 800°C and 900°C respectively.

Figure 6 shows the XRD pattern of $\text{Bi}_2\text{BaNa}_2\text{Nb}_4\text{O}_{15}$ precursor powder along with the precursor calcined at 800°C and 900°C respectively. Figure 6(a) shows the pattern for precursor powder. The pattern clearly shows that there are metal oxalate hydrates like barium oxalate hydrate $\text{BaC}_2\text{O}_4 \cdot 0.5\text{H}_2\text{O}$ (18-0184) and bismuth oxalate hydrate $\text{Bi}_2\text{C}_6\text{O}_{12} \cdot 7\text{H}_2\text{O}$ (38-0548), sodium niobium nitrate (72-1213) and unreacted niobium pentoxide Nb_2O_5 (34-1169).

Upon calcination at 800°C (Fig.6(b)) the major phases formed were BiNbO_4 and $\text{Ba}_5\text{Nb}_4\text{O}_{15}$. Other than these major phases bismuth and barium niobate phases were also identified in trace amount. The phases in 900°C (Fig.6(c)) calcined specimen were more or less similar to Fig.6(b), that is BiNbO_4 and BaNb_2O_6 phases were detected to be present in the system.

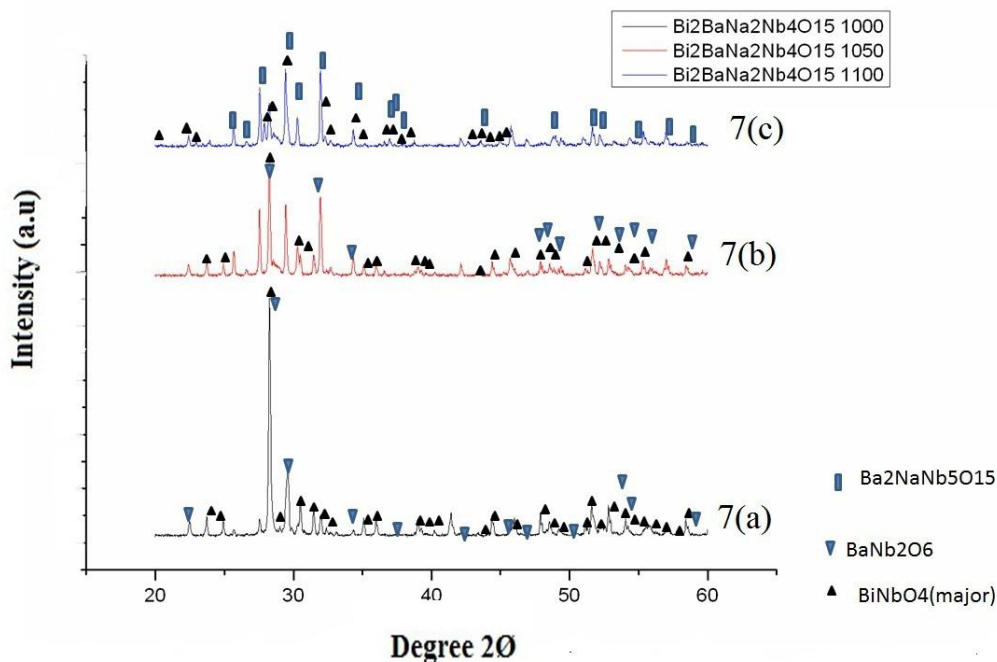


Figure 7: The XRD pattern of $\text{Bi}_2\text{BaNa}_2\text{Nb}_4\text{O}_{15}$ precursor powder along with the precursor calcined at 1000°C , 1050°C and 1100°C respectively.

Figure 7 shows the XRD pattern of precursor after 1000°C, 1050°C and 1100°C respectively. For all these specimens (Fig.7 (a), (b) and (c)), BiNbO₄ (16-0295) phases persisted. BaNb₂O₆ phase was present in 1000°C and 1050°C specimen. However from 1000°C onwards a new phase, Ba₂NaNb₅O₁₅ appeared in the specimen and finally after repeated calcination at 1100°C, the specimen showed to contain BiNbO₄ and Ba₂NaNb₅O₁₅ phases.

The desired Bi₂BaN_a₂Nb₄O₁₅ phase could not be achieved even after repeated calcinations. So long standing problem indicated previously that is the synthesis of 4-layered BLSF that contain both sodium and barium in B-site is a challenging task. The competing phase BiNbO₄ once produced in the system is more stable than the desired layered perovskite.

To avoid this it has been reported that [41] sodium niobate NaNbO₃ and Bi₂BaNb₂O₉ two layered aurivillius phase should be reacted to get the desired Bi₂BaN_a₂Nb₄O₁₅ phase.

So from this study it has been identified that BiNbO₄ phase must be avoided and accordingly the process parameters must be modified in future work.

4.2.2 Phase formation behavior of $\text{Bi}_2\text{CaNa}_2\text{Nb}_4\text{O}_{15}$.

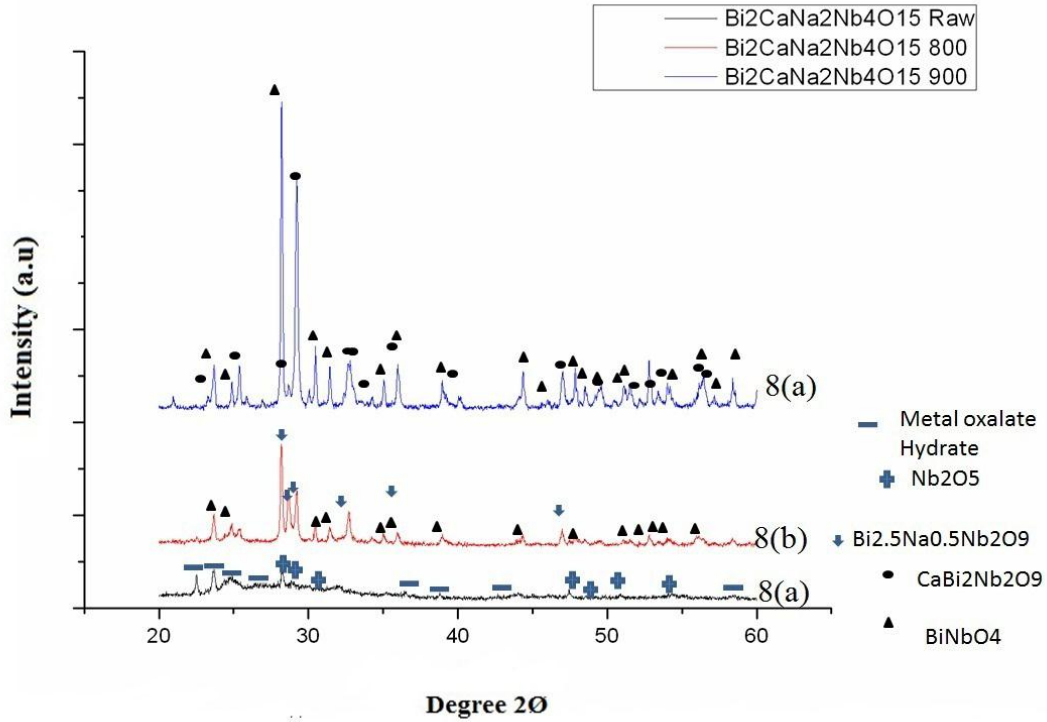


Figure 8: The XRD pattern of $\text{Bi}_2\text{CaNa}_2\text{Nb}_4\text{O}_{15}$ precursor powder and the precursor calcined at 800°C and 900°C respectively.

Figure 8 shows the XRD pattern of $\text{Bi}_2\text{CaNa}_2\text{Nb}_4\text{O}_{15}$ precursor powder along with the precursor calcined at 800°C and 900°C respectively. Figure 8(a) shows the XRD pattern of precursor powder. The pattern clearly shows the presence of metal oxalate hydrates like Calcium Oxalate Hydrate $\text{CaC}_2\text{O}_4 \cdot \text{H}_2\text{O}$ (01-0157) and Bismuth Oxalate Hydrate $\text{Bi}_2\text{C}_6\text{O}_{12} \cdot 7\text{H}_2\text{O}$ (38-0548) and unreacted Niobium Pentoxide Nb_2O_5 (34-1169).

After calcination at 800°C (Fig.8 (b)) the specimen shows formation of BiNbO_4 (16-0295) and $\text{CaBi}_2\text{Nb}_2\text{O}_9$ (72-2364) two layered perovskite which is desired for present synthesis. Similar two phases were also formed at 900°C (Fig.8(c)) calcined specimen.

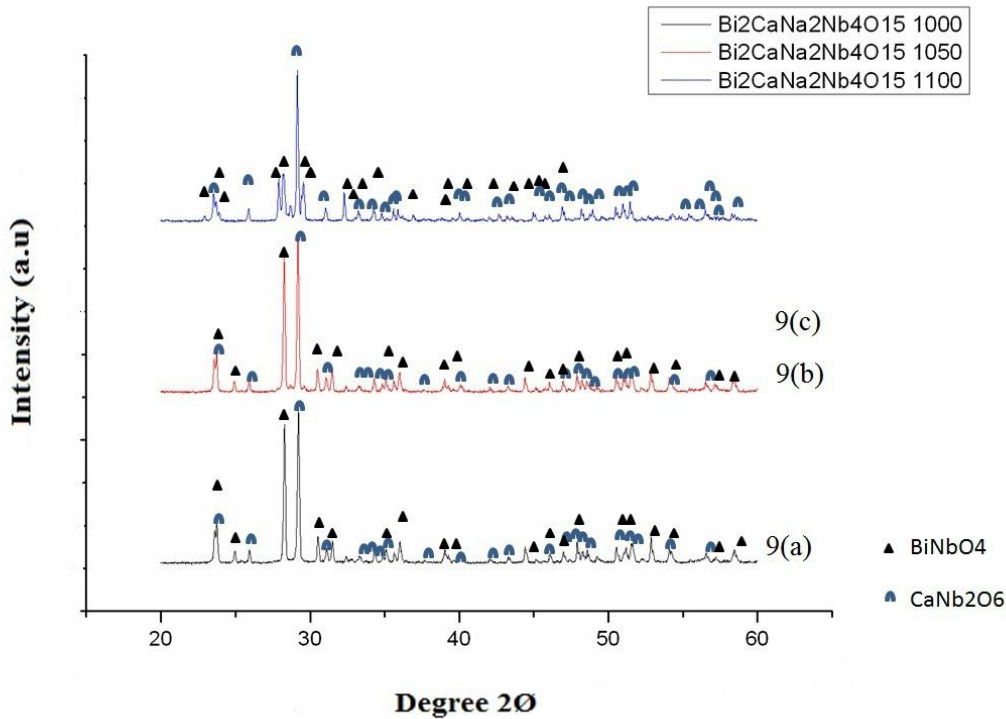


Figure 9: The XRD pattern of $\text{Bi}_2\text{CaNa}_2\text{Nb}_4\text{O}_{15}$ precursor powder and the precursor calcined at 1000°C, 1050°C and 1100°C respectively.

However at 1000°C (Fig.9(a)) the specimen shows the major phases as BiNbO_4 and CaNb_2O_6 i.e. there is decomposition of $\text{CaBi}_2\text{Nb}_2\text{O}_9$ which is harmful for this phase synthesis because the 1050°C (Fig.9(b)) and 1100°C (Fig.9(c)) powder also shows the presence of BiNbO_4 and CaNb_2O_6 . There was no further reaction in between these two phases. So it may be concluded that BiNbO_4 and CaNb_2O_6 are more stable than the four layered $\text{Bi}_2\text{CaNa}_2\text{Nb}_4\text{O}_{15}$. So the processing must be made in such a way that the formation of these two phases must be restricted.

One of the mechanisms may be by restricting the processing temperature below 1000°C as per results.

4.2.3 Phase formation behavior of $\text{Bi}_2\text{SrNa}_2\text{Nb}_4\text{O}_{15}$.

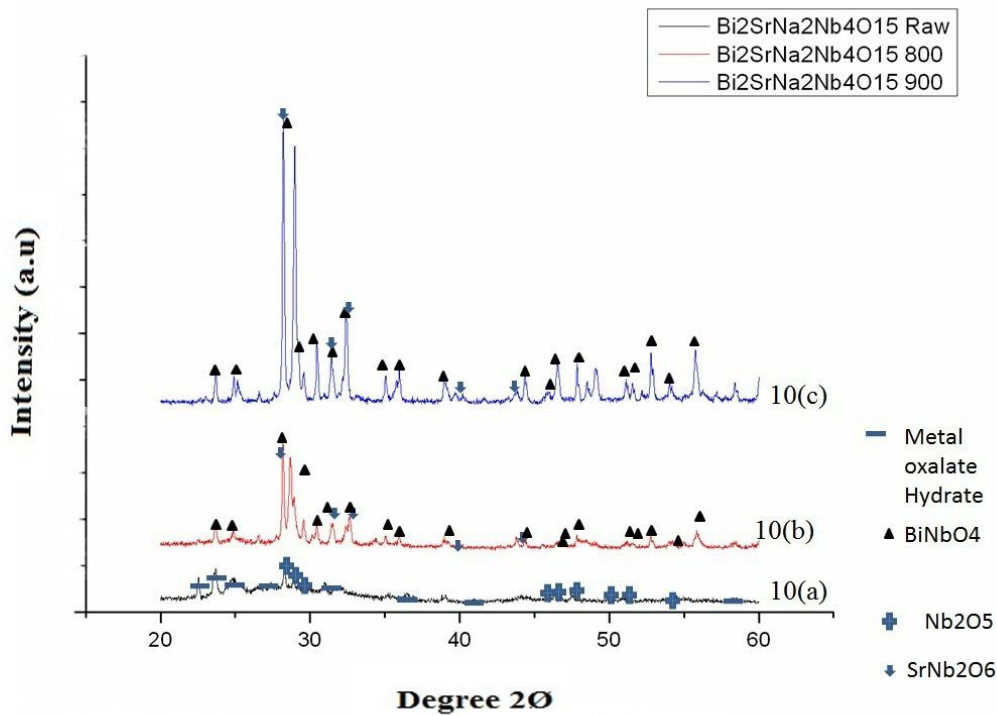


Figure 10: The XRD pattern of $\text{Bi}_2\text{SrNa}_2\text{Nb}_4\text{O}_{15}$ precursor powder and the precursor calcined at 800°C and 900°C respectively.

Figure 10 shows the XRD pattern of $\text{Bi}_2\text{SrNa}_2\text{Nb}_4\text{O}_{15}$ precursor powder along with the precursor calcined at 800°C and 900°C respectively. Figure 10(a) shows the pattern for precursor powder. The pattern clearly shows the presence of BiNbO_4 and unreacted Niobium Pentoxide Nb_2O_5 (34-1169).

After calcination at 800°C the major phase formed were strontium niobate and BiNbO₄. At 900°C similar phases were found but with different stoichiometric composition of strontium niobate like Sr₂Nb₂O₇ and Sr₅Nb₄O₁₅.

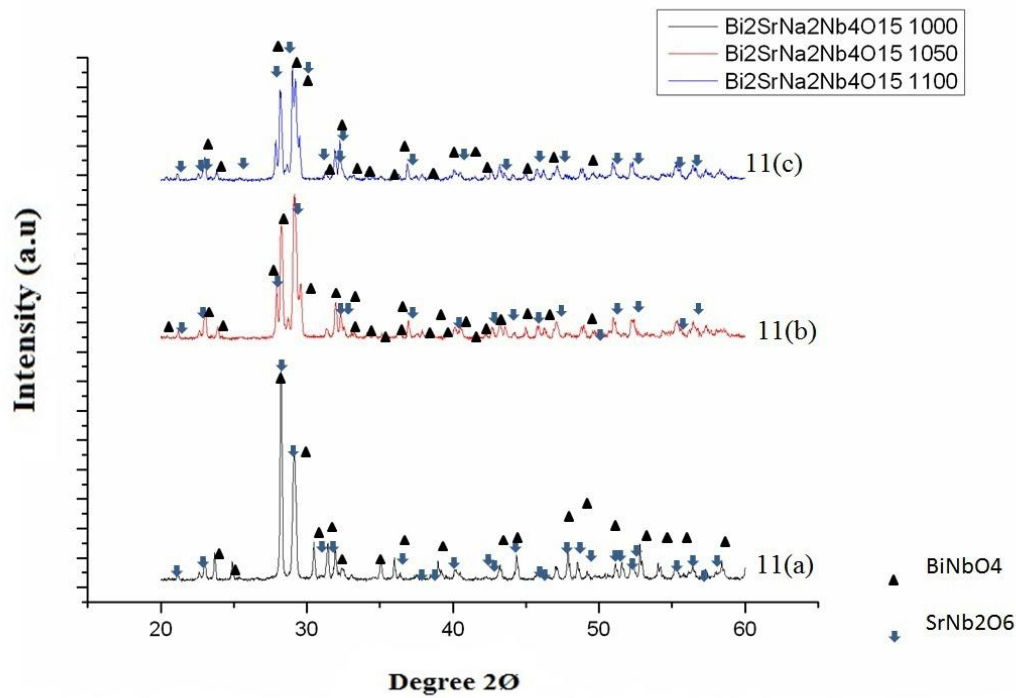


Figure 11: The XRD pattern of Bi₂SrNa₂Nb₄O₁₅ precursor powder and the precursor calcined at 1000°C, 1050°C and 1100°C respectively.

However at 1000°C (Fig.11(a)) and above again the major phase were SrNb₂O₆ and BiNbO₄. So the reaction mechanism for this case of more problematic for final phase synthesis. Once SrNb₂O₆ and BiNbO₄ were produced in the system, they were very stable compared to 4-layered Aurivillius compounds. So formation of these two phases must be avoided.

CHAPTER 5

CONCLUSIONS

Conclusion

In summary, $\text{Bi}_2\text{MNa}_2\text{Nb}_4\text{O}_{15}$ ($\text{M} = \text{Ca}, \text{Sr}, \text{Ba}$) phase was synthesized by Oxalate precipitation route. The XRD pattern of the final calcined specimen showed the presence of the parent $\text{Bi}_2\text{MNa}_2\text{Nb}_4\text{O}_{15}$ ($\text{M} = \text{Ca}, \text{Sr}, \text{Ba}$) phase and also presence of secondary phase of BiNbO_4 . On repetitive calcinations of the precursor powder, the metal oxalate hydrates and later on metal niobates were obtained out of which the BiNbO_4 was the competing phase that did not allow the formation of the desired phase. In case of calcium based precursor powder ($\text{Bi}_2\text{CaNa}_2\text{Nb}_4\text{O}_{15}$) the starting material that is $\text{CaBi}_2\text{Nb}_2\text{O}_9$ (72-2364), two layered perovskite was obtained which later decomposed at 1000°C ($\text{CaBi}_2\text{Nb}_2\text{O}_9$). This proved that the working temperature limit for these types of compounds should be within 1000°C .

REFERENCES

References

- [1] B. Aurivillius, *Ark. Kemi* 1 (1949) 463–480.
- [2] B. Aurivillius, *Ark. Kemi* 1 (1949) 499–512.
- [3] B. Aurivillius, *Ark. Kemi* 2 (1950) 519–527.
- [4] C. A-Paz de Araujo, J.D. Cuchiaro, L.D. Mcmillan, M.C. Scott and J.F. Scott, *Nature* 374 (1995), p. 627.
- [5] B.H. Park, B.S. Kang, S.D. Bu, T.W. Noh, J. Lee and W. Jo, *Nature* 401 (1999), p. 682.
- [6] R.K. Graselli, *Top. Catal.* 21 (2002), p. 79.
- [7] R. Funahashi, I. Matsubara and S. Sodeoka, *Appl. Phys. Lett.* 76 (2000), p. 2385.
- [8] L.T. Sim, C.K. Lee and A.R. West, *J. Mater. Chem.* 12 (2002), p. 17.
- [9] R.E. Newnham, R.W. Wolfe and J.F. Dorrian, *Mater. Res. Bull.* 6 (1971), p. 1029
- [10] E.C. Subarao, *J. Am. Ceram. Soc.* 45 (1962), p. 166.
- [11] H. Ogawa, M. Kimura, A. Ando and Y. Sakabe, *J. Appl. Phys.* 40 (2001), p. 5715.
- [12] A. Kingon, *Nature* 401 (1999) 658–659.
- [13] S. Ida, C. Ogata, U. Unal, K. Izawa, T. Inoue, O. Altuntasoglu, Y. Matsumoto, *J. Am. Chem Soc.* 129 (2007) 8956–8957
- [14] R.E. Schaak, T.E. Mallouk, *Chem. Commun.* (2002) 706–707.
- [15] M. Kudo, H. Ohkawa, W. Sugimoto, N. Kumada, Z. Liu, O. Terasaki, Y. Sugahara, *Inorg. Chem.* 42 (2003) 4479–4484.

- [16] S. Taharaa, A. Shimadaa, N. Kumadab, Y. Sugahara, *J. Solid State Chem.* 180 (2007) 2517–2524.
- [17] E.E. McCabe, C. Greaves, *J. Mater. Chem.* 15 (2005) 177–182.
- [18] N.A. Hill, *J. Phys. Chem. B* 104 (2000) 6694–6709
- [19] H.G. Kim, D.W. Hwang, J.S. Lee, *J. Am. Chem. Soc.* 126 (2004) 8912–8913.
- [20] M. Kudo, S. Tsuzuki, K. Katsumata, A. Yasumori, Y. Sugahara, *Chem. Phys. Lett.* 393 (2004) 12–16.
- [21] H.G. Kim, O.S. Becker, J.S. Jang, S.M. Ji, P.H. Borse, J.S. Lee, *J. Solid State Chem.* 179 (2006) 1214–1218.
- [22] J.C. Jung, H. Lee, H. Kim, Y.M. Chung, T.J. Kim, S.J. Lee, S.H. Oh, Y.S. Kim, I.K. Song, *J. Mol. Catal. A: Chem.* 271 (2007) 261–265.
- [23] Y. Shimodaira, H. Kato, H. Kobayashi, A. Kudo, *J. Phys. Chem. B* 110 (2006) 17790–17797.
- [24] A.M. la Cruz, S.O. Alfaro, E.L. Cuellar, U.O. Mendez, *Catal. Today* 129 (2007) 194–199.
- [25] L.S. Zhang, W.Z. Wang, L. Zhou, H.L. Xu, *Small* 3 (2007) 1618–1625.
- [26] L.S. Zhang, W.Z. Wang, Z.G. Chen, L. Zhou, H.L. Xu, W. Zhu, *J. Mater. Chem.* 17 (2007) 2526–2532.

- [27] H.B. Fu, L.W. Zhang, W.Q. Yao, Y.F. Zhu, *Appl. Catal. B: Environ.* 66 (2006) 100–110.
- [28] J. Wu, F. Duan, Y. Zheng, Y. Xie, *J. Phys. Chem. C* 111 (2007) 12866–12871.
- [29] J. Tellier, Ph. Boullay, M. Manier, D. Mercurio, *J. Solid State Chem.* 177 (2004) 1829–1837.
- [30] C. Miranda, M.E.V. Costa, M. Avdeev, A.L. Kholkin, J.L. Baptist, *J. Eur. Ceram. Soc.* 21 (2001) 1303–1306 .
- [31] G.C.C. da Costa, A.Z. Simoes, A. Ries, S.R. Foschini, M.A. Zaghete, J.A. Varela, *Mater. Lett.* 58 (2004) 1709–1714.
- [32] Jenny Tellier a, Philippe Boullay a,* , Dorra Ben Jennet b, Daniele Mercurio a *Solid State Sciences* 10 (2008) 177e185
- [33] A. Vadivel Murugan, S.C. Navale and V. Ravi *Materials Letters* Volume 60, Issue 8, April 2006, Pages 1023-1025
- [34] Dan Xie' and Wei Pan *Materials Letters* Volume 57, Issue 19, June 2003, Pages 2970-2974
- [35] Irena Pribošič, Darko Makovec, Miha Drogenik *Article Journal of the European Ceramic Society*, Volume 21, Issues 10-11, 2001, Pages 1327-1331

- [36] J Tellier, Ph Boullay, M Manier, D Mercurio Original Research Article Journal of Solid State Chemistry, Volume 177, Issue 6, June 2004, Pages 1829-1837
- [37] R.Z.Hou, X.M.Chen Original Research Article Solid State Communications, Volume 130, Issue7,May2004,Pages469-472.
- [38] Brendan J. Kennedy, Qingdi Zhou, Ismunandar, Yoshika Kubota, Kenichi Kato Journal of Solid State Chemistry 181 (2008) 1377–1386
- [39] W. Sugimoto, M. Shirata, Y. Sugahara, K. Kuroda, J. Am. Chem. Soc. 121 (1999) 11601–11602.
- [40] W. Sugimoto, M. Shirata, K. Kuroda, Y. Sugahara, Chem. Mater. 14 (2002) 2946–2952.
- [41] Zhenhua Liang, Kaibin Tang,_, Suyuan Zeng, Dong Wang, Tanwei Li, Huagui Zheng Journal of Solid State Chemistry 181 (2008) 2565– 2571
- [42] Chakrabarti. A , Bera J , Sinha T.P Physica B 404 (2009) 1498–1502.